

Analysis of Kinetics Parameters of Oil Shale Pyrolysis

Juliana P. Foltin*, Guilherme N. Prado, Antonio C. L. Lisbôa

Department of Process Engineering, State University of Campinas, City University Zeferino Vaz, Av. Albert Einstein, 500 – Zip Code: 13083-852 - Campinas - SP – Brazil.
juliana.p.foltin@gmail.com

The composition of the shale is a mixture of kerogen contained in the shale of organic matter and various mineral compounds. The limits between the kerogen and the mineral compounds can only be broken by the pyrolysis process, being very complex due to the structure of the kerogen generating many reactions. These reactions involve the breaking of chemical bonds with different energies in the organic phase and between the organic phase and the mineral matter. New alternatives are being studied for oil recovery between the use of shale. As a new requirement of an alternative for improvements in shale processing, is to optimize the pyrolysis process, through literature models are calculated kinetic parameters. Thus, kinetic parameters were determined from dynamic thermogravimetric analysis (TGA) in the temperature range of 323 K to 1,173 K, using different methods proposed by the literature. One of the most common places for extracting bituminous shale is the Irati basin in southern Brazil. The extraction was carried out by Petrobras / SIX in the city of São Mateus do Sul, Parana, Brazil. The kinetic parameters, as well as the activation energy and the pre-exponential factor were calculated using Friedman, Kissinger, Kissinger-Akahira-Sunose (KAS) methods and the Flynn-Wall-Ozawa (FWO) method. In addition, it was studied the characterization of shale behavior for a better evaluation.

1. Introduction

According to Müller et al. (2014), in the recent years an extensive exploration for oil shale has been done to replace oil as a second energy source. The oil shale is sedimentary rock with a mixture of mineral particles and organic matter in their midst. The origin of oil shale impacts provides to it significant differences in composition and proportions of minerals and organic matter. As commented before, the use of oil shale may drive the reduction of conventional energy resources and reduce energy prices. In this scenario, the use of oil shale from petroleum and the development of effective and economical techniques for the recovery of shale have been evaluated by many countries and shale (Dai et al., 2015).

In general, the shale pyrolysis process involves quite complex physical and chemical reactions. Aiming to improve reaction conditions of shale pyrolysis processes, experimental studies have been conducted to increase the understanding the impacts of variations in composition of the oil shale into fundamental process parameters. These studies encompass material composition, particle size, mineral matrix, pyrolysis temperature, heating rate, residence time for the pyrolysis reaction and pyrolysis atmosphere composition, (Lin et al., 2017).

To describe the shale formation, geologically speaking, is important to raise that although their different formations they have some similarities. (George, 1925) comments the low performance of the organic component (kerogen) on solvent solubility despite the possibility to recover oil from the kerogen by pyrolysis. According to Knaus (2010), basins are widespread throughout the world with the bigger deposits located in the United States, Russia, Congo and Brazil. According to (Boak, 2014), mining and in situ recovery methods are used for oil shale and the kerogen have some particularities that do not allow an effective extraction at moderate temperatures using water or organic solvents asking for temperatures higher than 573K to recover the oil shale.

Hubbard and Robinson (1950) presented the kinetics of devolatilization which can be analyzed including an induction period in thermal analysis of data. The International Confederation of Thermal Analyses and Calorimetry (ICTAC) inferred that the isoconversional methods are adequate to evaluate the Kinect of fossil

fuels, once they present a relation between the process temperature and the conversion rate, without considering a reaction model (Bai et al., 2015).

According to Tiwari and Deo (2012), TGA has been successfully employed for the study of the pyrolysis kinetics with various shales. The data were modeled using model-free and model-fitting approaches in order to evaluate the activation energy and the pre-exponential factor. This was followed by a critical evaluation of the kinetics and the implications for practical use in the design of oil shale pyrolysis processes.

2. Materials and Methods

For this study, the shale used was extracted from the Irati Formation and supplied by Petrobras / SIX, located in Sao Mateus Do Sul, Parana, Brazil, with particle range size – 42 Mesh + 48 Mesh (0.354 mm to 0.297 mm). Parameters kinetics as activation energy (E) and the pre-exponential factor (k_0) were determined using thermogravimetric analyser (TGA). For analysis 9.5 mg of shale was weighed and put inside alumina crucible. All the analyses were performed using the equipment model TGA/DSC1 with a microbalance model MX5 of measuring range 5 g and resolution 1 μ g and Stare software from Mettler Toledo. The sample was heated under nitrogen flow of 50 ml/min, atmosphere since 373K to 1,173K, at different heating rates (β): 2, 5, 10, 15, 20, 25, 40 and 50 K/min. The final material was considered to be ash (oxidized mineral matter), i.e. all material that did not form gaseous combustion products.

3. Model-Free

Kinetics parameters were determined by relating the mass loss versus temperature response at different heating rates to the oil shale pyrolysis kinetics. The kinetics of decomposition analysis are based on the Arrhenius equation Eq(1), and kerogen transformation rate for the volatile product Eq(2):

$$k = k_0 \cdot e^{\left(\frac{-E}{RT}\right)} \quad (1)$$

$$\frac{d\alpha}{dt} = k(T) \cdot f(\alpha) \quad (2)$$

In these equations k is the rate constant, k_0 is the pre-exponential factor, E is the activation energy. The conversion α , is the standard form of the sample mass loss and is defined according to Eq(3), in which m_f is the mass remaining after pyrolysis at 1,173 K (i.e. not conversion expressed in terms of the Fischer assay procedure, Lee (1991).

$$a = \frac{m_o - m}{m_o - m_f} \quad (3)$$

The combination of Eq(1) and Eq(2) provides the fundamental expression, Eq(4), which is based on analytical methods to calculate the kinetic parameters based on results of TGA.

$$\frac{d\alpha}{dt} = k_0 \cdot f(\alpha) \cdot e^{\left(\frac{-E}{RT}\right)} \quad (4)$$

The function f (α), Eq(5) is inserted into Eq(4), producing Eq(6), wherein the parameter $\beta = dT / dt$, the heating rate, is used:

$$f(\alpha) = (1 - \alpha)^n \quad (5)$$

$$\frac{d\alpha}{dT} = \frac{k_0}{\beta} (1 - \alpha)^n \cdot e^{\left(\frac{-E}{RT}\right)} \quad (6)$$

Four different methods were employed to calculate the pyrolysis kinetics from the TGA data, namely, Friedman, Flynn–Wall–Ozawa, Kissinger–Akahira–Sunose, and Kissinger. The methods were associated with model-free descriptions of the kinetics presents in Table 1.

Table 1: Approximate equations of the kinetic methods. Adapted from (Bai et al., 2015)

Methods	Equation	X	Y
Friedman	$\ln \frac{d\alpha}{dt} = \ln[k_0 \cdot f(\alpha)] - \frac{E}{RT}$	$\frac{1000}{T}$	$\ln\left(\frac{d\alpha}{dt}\right)$
FWO	$\ln(\beta_i) = \ln\left(\frac{k_0 \cdot E}{R \cdot g(\alpha)}\right) - 5.331 - 1.052 \frac{E}{RT}$	$\frac{1000}{T}$	$\ln(\beta_i)$
Kissinger	$\ln\left(\frac{\beta}{T_m^2}\right) = \ln\left(\frac{k_0 \cdot R}{E}\right) - \frac{E}{RT_m}$	$\frac{1000}{T}$	$\ln\left(\frac{\beta}{T_m^2}\right)$
KAS	$\ln\left(\frac{\beta}{T^2}\right) = \ln\left(\frac{k_0 \cdot R}{E \cdot g(\alpha)}\right) - \frac{E}{RT}$	$\frac{1000}{T}$	$\ln\left(\frac{\beta}{T^2}\right)$

4. Results

According to Figure 1, the pyrolysis process presents two phases that will be identified as Region II and III. In Region II we can identify the main parameters, as temperature at maximum mass loss and Region Initial Temperature, for each heating rate which will allow the calculation of the Kinect parameters. In Table 2 are listed the Initial Temperature (T_i), the Maximum temperature conversion (T_{max}) and the Maximum Conversion at T_{max} (α_{max}) for each of these two phases.

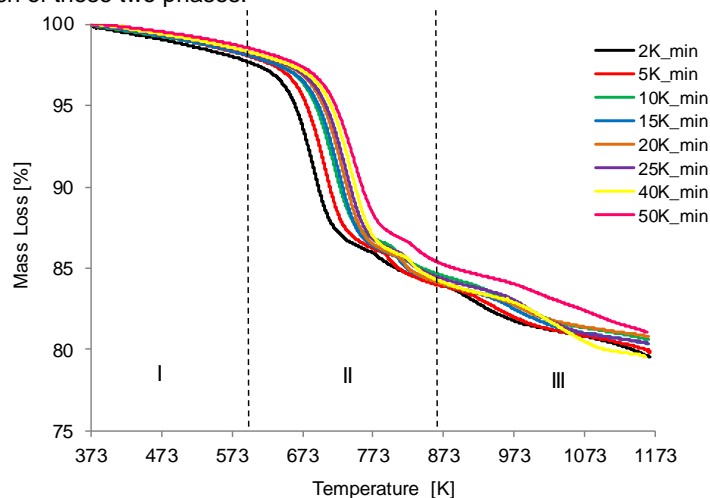


Figure 1: Mass Loss between 373 to 1,173K obtained from TGA.

Once the Heating Rate increases, the Initial Temperature observed in Region II increases, being constant at 693K for heating rates above 20 K/min. This behavior is also seen for the Maximum Conversion Temperature, which increases uniformly according to the increase of heating rate, although the conversion at this temperature remains between 0.42 and 0.47.

In Region III, the Initial Temperature and the Maximum Conversion Temperature have the same behavior as observed in Region II. In Region III, in temperatures above 1,173 K the total conversion remains constant between 19.9 % to 20.5 % in mass independently of the heating rate. No specific tendency is observed between the total mass loss and the heating rate. This is a critical observation due to the fact that, at a low heating rates, the production of oil is affected when the pyrolysis ends at low temperatures, as observed into the practical pyrolysis operation (Burnham, 2010).

Table 2 – Data of temperature for decomposition and rapid pyrolysis

Phase	Heating rate (K/min)	2	5	10	15	20	25	40	50
Decomposition	Initial Temperature (K)	608	638	672	677	690	689	688	689
	Maximum Conversion Temperature (K)	687	706	717	720	729	734	741	748
	Maximum Conversion at T_{max} (%)	41.8	45	44	42.9	46.6	46	44	46
Rapid Pyrolysis	Initial Temperature (K)	763	784	796	804	805	810	816	820
	Maximum Conversion Temperature (K)	782	794	804	810	813	820	826	831
	Maximum Conversion at T_{max} (%)	70	71.2	71.3	73.8	75.4	73.5	71.2	72.2

Figures 2, 3, 4 and 5 show the graphs of several Model-Free models with conversions range of 0.15 and 0.65. The temperature at which the reaction occurs has the same range of this conversions range and this was the main reason to select them.

The calculations of kinetic parameters were done in accordance with each Model-Free model based on the data obtained from the TGA.

By the methods Friedman, KAS and FWO, the activation energy (E) and the pre-exponential factor (k_0) were obtained and the calculations were made according to equations in Table 1. The activation energy (E) and the pre-exponential factor (k_0) were obtained by the linear regression and calculating the slope and intercept, respectively. The results are shown in Table 3.

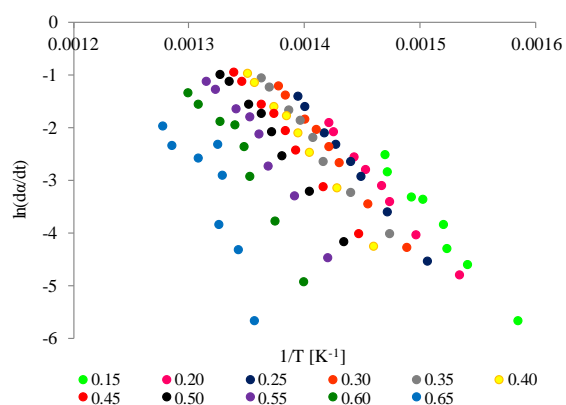


Figure 2: Method of Friedman for different conversions.

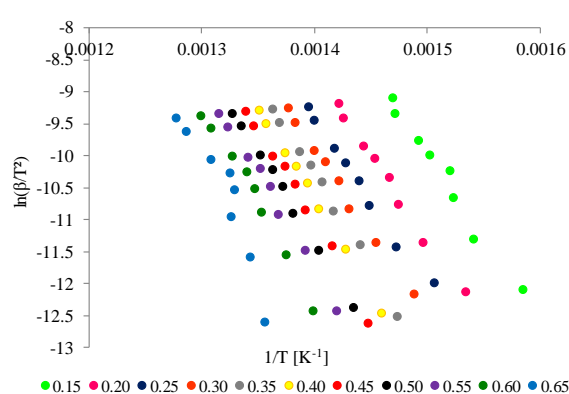


Figure 4: Method of Kissinger-Akahira-Sunose for different conversions.

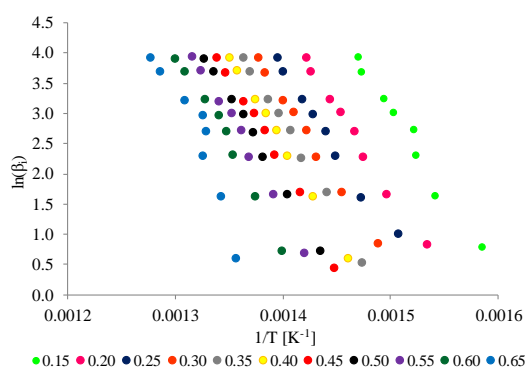


Figure 3: Method of Flynn-Wall-Ozawa for different conversions.

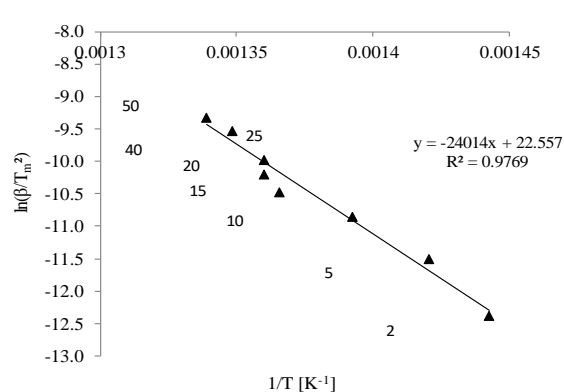


Figure 5: Method of Kissinger for different heating rates.

The pyrolysis kinetic has as directly relation with the conversion rate as presented in Table 3. Although a progressive increase of the activation energy with the conversion is observed, several authors present overall values for the activation energy between 215 kJ mol⁻¹ and 255 kJ mol⁻¹, considering the conversion range of 0.15 ≤ α ≤ 0.55.

Table 3: Parameters values for E and k₀ calculated

A	Friedman			FWO			KAS		
	E	k ₀	r ²	E	k ₀	r ²	E	k ₀	r ²
0.05	143.2	2.66E+12	0.773	120.9	1.01E+11	0.895	118.7	5.27E+10	0.881
0.10	141.5	2.10E+10	0.955	179.7	2.71E+14	0.895	179.0	2.27E+14	0.884
0.15	221.3	8.05E+15	0.982	215.9	1.68E+16	0.977	216.2	1.72E+16	0.975
0.20	216.6	2.09E+15	0.995	218.9	1.03E+16	0.993	219.0	1.02E+16	0.992
0.25	231.8	2.45E+16	0.999	211.5	1.78E+15	0.990	211.0	1.58E+15	0.989
0.30	234.0	3.02E+16	0.998	218.4	4.60E+15	0.996	218.2	4.25E+15	0.995
0.35	228.1	9.40E+15	0.995	239.7	1.45E+17	0.995	240.4	1.58E+17	0.995
0.40	248.7	2.44E+17	0.994	239.2	1.09E+17	0.998	239.8	1.17E+17	0.998
0.45	239.7	4.42E+16	0.995	246.3	2.99E+17	0.992	247.2	3.34E+17	0.991
0.50	253.0	2.98E+17	0.988	236.6	4.79E+16	0.997	236.9	4.83E+16	0.996
0.55	269.5	2.99E+18	0.969	245.3	1.65E+17	0.992	245.9	1.76E+17	0.992
0.60	299.7	2.04E+20	0.931	254.7	5.63E+17	0.982	255.6	6.30E+17	0.981
0.65	328.2	4.56E+21	0.703	301.1	5.56E+20	0.868	304.1	8.34E+20	0.858

Table 4 presents the data calculated from the Kissinger model equation. The Figure 5 shows a linear behavior in which the results are calculated from different heating rates.

Table 4: Kinetic parameters calculated by the Kissinger method

Equation	k ₀	E
y = - 24014.2 x + 22.56	1.50E+14	199.65

5. Conclusions

The kinetics based on Model-Free methods was measured experimentally during isothermal pyrolysis at 673K. The reaction rate calculated using kinetic parameters obtained by the Friedman method was more accurate than the other methods for lower conversion rates. The kinetic parameters calculated by the Flynn-Wall-Ozawa and Kissinger-Akahira-Sunose methods became more accurate in higher conversion rate. In general, the Friedman method underestimated the reaction rate observed at 673 K, while the Flynn-Wall-Ozawa, Kissinger-Akahira-Sunose and Kissinger methods overestimated the reaction rate. Isothermal pyrolysis presented an incomplete conversion limit with the increment of the temperature. This type of behavior was predicted by the conversion dependence of the activation energy.

Nomenclature

E	activation energy (kJ/mol)
f(α)	reaction model
k	reaction rate constant (units depend on reaction order)
k ₀	pre-exponential factor (min ⁻¹ for 1 st order)
m	mass of oil shale (mg)
m ₀	mass of oil shale before pyrolysis (mg)
m _f	mass of oil shale after pyrolysis (mg)
n	reaction order
r ²	determination coefficient
R	universal gas constant (J/mol·K)
t	time (min)
T	temperature (K)
α	kerogen conversion as defined by Eq(3) (mg/mg)
β	heating rate (K/min)

Acknowledgments

This study was funded through the program "Science Without Borders", the University of Alberta, and the State University of Campinas.

References

- Bai F., Guo W., Lü X., Liu Y., Guo M., Li Q., Sun Y., 2015. Kinetic study on the pyrolysis behavior of Huadian oil shale via non-isothermal thermogravimetric data, *Fuel*, 146, 111-118.
- Boak J., 2014. Shale-hosted hydrocarbons and hydraulic fracturing. In *Future Energy Improved, sustainable and clean options for our planet, 2ed*; Letcher, T. M. Ed.; Elsevier: Amsterdam, the Netherlands, 117-143.
- Burnham, A.K., 2015. A simple kinetic model of oil generation, vaporization, coking, and cracking, *Energy Fuels*, 29, 7156-7167.
- Cane R.F., Yen T.F., Chilingarian, G.V. 1976. The origin and formation of oil shale. In *Oil Shale*, Eds.; Elsevier: Amsterdam, 27-60.
- Duncan D.C., 1994. Geological setting of oil-shale deposits and world prospects. In *Oil shale*; Yen, T. F., Chilingarian, G. V. Eds.; Elsevier: Amsterdam, The Netherlands, 13-26.
- George R.D., 1925 Origin of oil shales. In *Shale oil (ACS Monograph Ser. 25)*; McKee, R. H. Ed.; Chemical Catalogue Company: New York, USA.
- Hillier J.L., Fletcher T.H., 2011, Pyrolysis kinetics of a Green River oil shale using a pressurized TGA, *Energy Fuels*, 25, 232-239.
- Hubbard A.B., Robinson W. E., 1950, A Thermal Decomposition Study of Colorado Oil Shale, USA Bureau of Mines Report of Investigations, 4744, p. 24.
- Janković B., 2013, The kinetic modeling of the non-isothermal pyrolysis of Brazilian oil shale: Application of the Weibull probability mixture model. *Journal of Petroleum Science and Engineering*, 111, 25-36.
- Knaus E., Killen J.; Biglarbigi K., Crawford P., 2010, An overview of oil shale resources. *ACS Symposium Series*, 1032, 3-20.
- Müller C.M., Pejčić B. Esteban L. Piñe, C B., Raven M., Mizaikoff B., 2014, Infrared Attenuated Total Reflectance Spectroscopy: An Innovative Strategy for Analyzing Mineral Components in Energy Relevant Systems, *Scientific Reports*.
- Lee S., 1991, *Oil Shale Technology*; CRC Press: Boca Raton, Florida, USA.
- Pan L., Dai F., Li G., Liu S., 2015, A TGA/DTA-MS investigation to the influence of process conditions on the pyrolysis of Jimsar oil shale. *Energy*, 86, 749-757.
- Saif T., Lin Q., Bijeljic B., Blunt M.J., 2017, Microstructural imaging and characterization of oil shale before and after pyrolysis, *Energy*, 197, 562-574.
- Tiwari P., Deo M., 2012, Compositional and kinetic analysis of oil shale pyrolysis using TGA-MS, *Fuel*, 94, 333-341.